INVESTIGATION OF THE INFLUENCE OF BUBBLE-BUBBLE INTERACTIONS ON THE HYDRODYNAMICS OF BUBBLING GAS-SOLID FLUIDISED BEDS USING THE DISCRETE BUBBLE MODEL

J.A. Laverman, M. van Sint Annaland, J.A.M. Kuipers

[1] University of Twente, P.O. Box 217, 7500 AE Enschede, The Netherlands

[2] Dutch Polymer institute (DPI), P.O.Box 902, 5600 AX Eindhoven, The Netherlands

ABSTRACT

To investigate the hydrodynamic behaviour of industrial scale bubbling fluidised bed reactors, a 3D Discrete Bubble Model (DBM) has been developed. In the DBM, an Euler-Lagrange model, the bubbles are treated as discrete elements and the bubble trajectories are tracked individually, while the emulsion phase is considered as a continuum and is described with the continuity and Navier-Stokes equations. The main advantage of the DBM is that it fully accounts for the two-way coupling, allowing computation of the prevailing macroscopic circulation patterns in large scale gas-fluidised beds. In this paper, we have examined the effect of bubble-bubble (wake) interactions on the macro-scale velocity profiles using the DBM. It has been found that the extent of the macroscopic circulation is significantly increased by the bubble-bubble interaction forces.

NOMENCLATURE

C	closure	[-]
D	distribution function	[m^{-1}]
F	force	[N]
g	gravitational acceleration	[m.s^{-2}]
l	bubble-bubble interaction coefficient	[-]
m	bubble-bubble interaction coefficient	[-]
m	mass of a bubble	[kg]
NX	number of grid cells in x-direction	[-]
NY	number of grid cells in y-direction	[-]
NZ	number of grid cells in z-direction	[-]
P	pressure	[Pa]
R	radius of bubble	[m]
t	time	[s]
U	emulsion phase velocity	[m.s^{-1}]
V	volume	[m^3]
v	bubble velocity	[m.s^{-1}]
x	x-position	[m]
y	y-position	[m]
z	z-position	[m]
ε	volume fraction	[-]
ρ	density	[kg.m^{-3}]
τ	stress tensor	[Pa]
Φ	source term	[N.m^{-3}]

Subscript

b	bubble
d	distance or drag
e	emulsion
g	gravitational
p	pressure
tot	total
vm	virtual mass
x	x-direction
y	y-direction
z	z-direction
1	leading bubble
2	tailing bubble
∞	velocity of a undisturbed bubble

INTRODUCTION

Bubbling gas-solid fluidised beds have found widespread application in the chemical process industries. An important process based on gas-solid fluidisation is the UNIPOL^{TM} process for the production of polyolefins such as polyethylene and polypropylene. This process uses highly active and selective catalysts, resulting in an enormous heat production, which needs to be removed from the fluidised bed reactor. The temperature of the reactor is not allowed to exceed the melting temperature of the polymer, because the polymer particles will start to melt and stick together. Despite the excellent heat transfer inside a fluidised bed, the heat removal rate limits the production capacity. One of the mechanisms with which heat is removed from the reactor is convective heat transfer via the emulsion phase. The convective heat transfer is mainly governed by the macroscopic circulation patterns that are largely induced by the bubbles. Therefore, quantitative information about the macroscopic circulation patterns of the emulsion phase is needed to improve the heat removal rate from the fluidised bed.

To describe the macroscopic circulation patterns prevailing in dense gas-solid fluidised bed reactors, a 3D Discrete Bubble Model (DBM) has been developed. In the DBM, an Euler-Lagrange model, the bubbles are modelled as discrete spherical elements and are tracked individually with Newton's second law during their rise through the emulsion phase. The emulsion phase is considered as a continuum, for which the continuity and Navier-Stokes equations are solved. In this paper, the influence of bubble-bubble interactions on the macro-scale circulation patterns in the emulsion phase is studied with the DBM.

DISCRETE BUBBLE MODEL

Although the DBM idealises the bubbles as perfect spheres, its strong advantage is that it fully accounts for the two-way coupling, i.e. the bubbles rising through the emulsion phase will affect the dynamics of the emulsion phase and, visa versa, the emulsion phase velocity patterns will be influenced by the drag exerted by the bubbles on the emulsion phase. In addition, the DBM requires no a priori assumptions on the encounter frequency, an important factor determining the bubble coalescence rate. A description of the DBM is given in this section, starting with the two phases of the fluidised bed reactor, the emulsion and bubble phase, then the coalescence of the bubbles, bubble-bubble interactions, the boundary conditions and finally the solution method are discussed.

Emulsion phase hydrodynamics

The emulsion phase consists of a mixture of particles and gas. The hydrodynamics of the emulsion phase is described in the DBM by the continuity equation and the volume-averaged Navier-Stokes equation.

$$\frac{\partial(\varepsilon_e\rho_e)}{\partial t} + \nabla\cdot\varepsilon_e\rho_e\mathbf{U} = 0$$
$$\frac{\partial(\varepsilon_e\rho_e\mathbf{U})}{\partial t} + \nabla\cdot\varepsilon_e\rho_e\mathbf{U}\mathbf{U} = -\varepsilon_e\nabla P - \nabla\cdot\varepsilon_e\tau_e + \varepsilon_e\rho_e\mathbf{g} + \Phi \quad (1)$$

The momentum transfer between the bubble and emulsion phase is described by the source term, Φ. The emulsion phase is assumed to behave like Newtonian fluid. The porosity of the emulsion phase is represented by ε_e, ρ_e is the emulsion phase density and g is the gravitational acceleration.

Bubble dynamics

The Lagrangian part of the model deals with the bubble phase. For each bubble, we solve the second law of Newton's second law, given by:

$$m_b\frac{d\mathbf{v}_b}{dt} = \sum\mathbf{F} = \mathbf{F}_g + \mathbf{F}_p + \mathbf{F}_d + \mathbf{F}_{vm} \quad (2)$$

where m_b and $\mathbf{v}_b$ respectively denote the bubble mass and velocity, $\mathbf{F}_g$, $\mathbf{F}_p$, $\mathbf{F}_d$ and $\mathbf{F}_{vm}$ are respectively, the gravitational, pressure, drag and virtual mass (added mass) force. The ODE's governing the motion of the bubbles are integrated in time using a simple first order scheme. Possible bubble-bubble and/or bubble-wall encounters are accounted for with an event-driven computational scheme. It has been assumed that there is no net gas exchange between the emulsion and bubble phase and that the bubbles only grow due to coalescence with other bubbles. The gravitational and pressure force can be added together to yield:

$$\mathbf{F}_g + \mathbf{F}_p = (\rho_e - \rho_g)V_b\mathbf{g} \quad (3)$$

where V_b is the volume of the bubble. The drag force is computed with the equation that Odar and Hamilton (1964) derived for spheres:

$$\mathbf{F}_d = -\frac{1}{2}C_D\pi R_b^2|\mathbf{U}-\mathbf{v}|(\mathbf{U}-\mathbf{v}) \quad (4)$$

Where C_D is the drag coefficient, R_b is the bubble radius, $\mathbf{U}$ and $\mathbf{v}$ are respectively, the emulsion phase and bubble velocity. In the drag coefficient the spherical cap shape of the bubble is implicitly accounted for. The last force that is incorporated in the DBM is the virtual mass force (Auton 1983), which is given by:

$$\mathbf{F}_{vm} = -\left(\frac{D\mathbf{I}}{Dt} - \mathbf{I}\cdot\nabla\mathbf{U}\right) \quad (5)$$

where

$$\mathbf{I} = C_{vm}\rho_e V_b(\mathbf{v}-\mathbf{U}) \quad (6)$$

where C_{vm} is the virtual mass constant and is assumed to be 0.5.

Bubble coalescence

As a first step, the description of bubble coalescence is simplified by assuming 100% coalescence efficiency for a bubble-bubble encounter, if the bubble diameter is smaller than the pre-described maximum bubble diameter. When a bubble encounters another bubble and would yield a bubble larger than the maximum bubble diameter upon coalescence, the bubbles do not coalesce but collide elastically, approximating the dynamic equilibrium between bubble break-up and bubble coalescence. More detailed closures for bubble coalescence and bubble break-up could in principle be easily implemented in the DBM. Due to the bubble coalescence, the bubbles can grow to diameters much larger than the size of an Eulerian grid cell required to accurately resolve the emulsion phase velocity patterns. The DBM, originally developed for and widely used in the field of gas-liquid columns, has been modified to cope with bubbles with a diameter much larger than the size of an Eulerian cell.

Bubble-bubble interaction

It is generally accepted that for fluidisation of Geldart B type solids, a large part of the gas is flowing from bubble to bubble through the bed. Due to this movement of the gas, an additional force is exerted on the bubble, here referred to as the bubble-bubble (wake) interaction. This force results in a higher bubble velocity and in a possible lateral movement of the bubble inside a fluidised bed reactor. Krishna and van Baten (2001) found that the bubble velocity was increased by a factor of 1.5 to 3 times the velocity of a single isolated bubble, showing the importance of the bubble-bubble interaction.
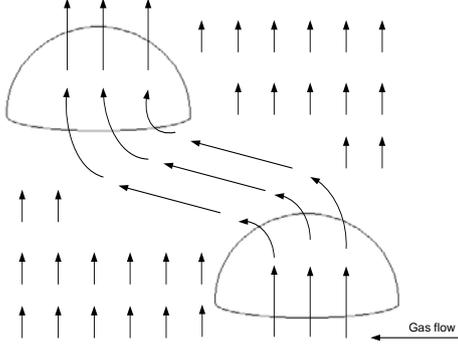
Figure 1: Schematic representation of the gas flow through a freely bubbling fluidised bed consisting of Geldart B type solids.

For the calculation of the bubble-bubble interaction forces, the model suggested by Farrokhalee (1979) has been implemented in the DBM. The difference between this model and the model suggested by Clift and Grace (1971) is that in the model developed by Farrokhalaee, the tailing bubble has no influence on the leading bubble. Clift and Grace (1985) confirmed that the simplification proposed by Farrokhalaee did not reduce the accuracy of the model and indicated that the experimental results could be equally well described. In this bubble-bubble interaction model, the velocity U_{i1} of the leading bubble remains the velocity of an undisturbed bubble $U_{i\infty1}$:

$$\begin{aligned} U_{z1} &= U_{z\infty1} \\ U_{x1} &= U_{x\infty1} \\ U_{y1} &= U_{y\infty1} \end{aligned} \qquad (7)$$

However, the velocity of a tailing bubble U_{i2} is affected (provided that the distance between the bubble centres is less than 5 bubble radii) according to:

$$\left.\begin{aligned} U_{z2} &= U_{b\infty2} + l_{2,1}U_{b\infty1} \\ U_{x2} &= m_{2,1,x}U_{b\infty1} \\ U_{y2} &= m_{21,y}U_{b\infty1} \end{aligned}\right\} \left[\left(x_d - R_2\right)^2 + y_d^2 > R_1^2 > 5R_1^2 \right]$$

$$\left.\begin{aligned} U_{z2} &= U_{z\infty2} \\ U_{x2} &= U_{x\infty2} \\ U_{y2} &= U_{y\infty2} \end{aligned}\right\} \left[\left(x_d - R_2\right)^2 + y_d^2 > 5R_1^2 \right] \qquad (8)$$

where xd and yd is the distances between the two bubbles in respectively the x- and y-direction. Johnsson proposed relations for the coefficients m2,1 and l2,1, which were described by Clift and Grace (1985). These coefficients have been extended to motion in three dimensions:

$$l_{2,1} = \frac{\left[2\left(z_2 - z_1 + R_2\right)^2 - \left(\sqrt{\left(x_2 - x_1\right)^2 + \left(y_2 - y_1\right)^2}\right)^2 \right] R_1^3}{2\left[\left(z_2 - z_1 + R_2\right)^2 + \left(\sqrt{\left(x_2 - x_1\right)^2 + \left(y_2 - y_1\right)^2}\right)^2 \right]^{\frac{5}{2}}} \qquad (9)$$

$$m_{2,1} = \frac{3\left(z_2 - z_1 + R_1\right)\left(\sqrt{\left(x_2 - x_1\right)^2 + \left(y_2 - y_1\right)^2}\right) R_1^3}{2\left[\left(z_2 - z_1 + R_1\right)^2 + \left(\sqrt{\left(x_2 - x_1\right)^2 + \left(y_2 - y_1\right)^2}\right)^2 \right]^{\frac{5}{2}}} \qquad (10)$$

where

$$\begin{aligned} m_{2,1,x} &= m_{2,1}\left(\frac{x_d}{\sqrt{x_d^2 + y_d^2}} \right) \\ m_{2,1,y} &= m_{2,1}\left(\frac{y_d}{\sqrt{x_d^2 + y_d^2}} \right) \end{aligned} \qquad (11)$$

As a first step, only binary interaction forces between a bubble and its nearest leading neighbour are considered. In future work, effects of multiple bubble-bubble interactions between different bubble pairs will be investigated.

Boundary conditions

Boundary conditions that are imposed on the walls utilise the matrix concept of Kuipers et al. (1993). The boundaries are schematically presented in Figure 2 and the corresponding boundary conditions are given in Table 1.
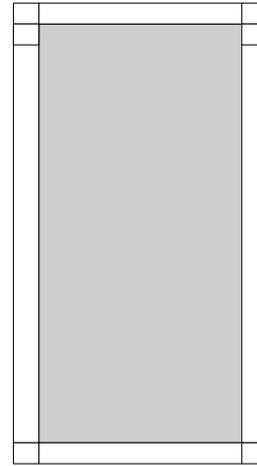
Figure 2: Flag matrix concept used in the flow solver.

flag	Boundary conditions
1	Interior cell, no boundary conditions
2	Impermeable wall, free slip boundary
3	Impermeable wall, no slip boundary
5	Prescribed pressure cell, free slip boundary
7	Corner cell, no boundary condition

Table 1: Cell flags and their corresponding boundary conditions.

The prescribed pressure cells near the top of the column serve as inlet and outlet zones to accommodate for the changes in the emulsion phase volume when the bubbles enter or leave the column (Darmana et al., 2005). During the initialisation step of the simulation the pressure is set to the hydrostatic pressure in the reactor. Initially the bubbles rise with the bubble velocity corresponding with the specified visible bubble flow rate. When the bubble touches the top boundary of the column, the bubble is marked to be removed from the column. When this happens, the velocity and the interphase momentum transfer to the emulsion phase are no longer updated and the bubble leaves the column with a constant velocity.

Solution method

The SIMPLE algorithm is used to solve for the pressure and velocity fields of the emulsion phase, which are described by the Navier-Stokes equation. To evaluate the convective terms in the continuity and momentum equations, a second order accurate Barton scheme is used, whereas the standard second order central discretisation is used for the diffusive terms. A first order implicit time integration is used to solve the force balance for every individual bubble in the fluidised bed.

The interaction between the bubble and the emulsion phase is calculated via the two-way coupling method. This means that the bubble phase affects the emulsion phase by the void fraction and the momentum transfer rate from the bubble to the emulsion phase, represented by the source term in the Navier-Stokes equation.

$$\Phi = -\frac{1}{V_{cell}} \sum_{\forall i \in cell} \left(\mathbf{F}_{d,i} + \mathbf{F}_{vm,i} \right) \qquad (12)$$

Furthermore, the emulsion phase influences the bubbles via the slip velocity in the drag and virtual mass forces. Because the bubbles can grow larger than the grid size, the volume averaging technique cannot be applied. To map the momentum of bubbles that are larger than a grid cell, a normalized polynomial distribution function is used to distribute the momentum over the surrounding cells and the same function is used to map the Eulerian information to the position of the bubble (Deen et al., 2004). The interested reader is referred to the article of Deen et al., (2004), for the specifics of the distribution function.

$$D\left(x_i - x_{i,b} \right) = \frac{15}{16} \left[\frac{\left(x_i - x_{i,b} \right)^4}{n^5} - 2\frac{\left(x_i - x_{i,b} \right)^2}{n^3} + \frac{1}{n} \right] \qquad (13)$$
$$-n \le \left(x_i - x_{i,b} \right) \le n$$

A complete description of the model can be found in (Bokkers, 2005) or (Bokkers et al., 2006).

RESULTS AND DISCUSSION

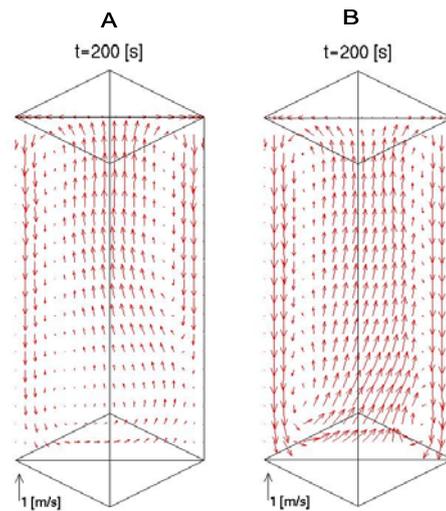### Influence of bubble-bubble interaction

To investigate the influence of bubble-bubble interaction on the macroscale circulation patterns, two simulations have been performed, where, in the first simulation the bubble-bubble interaction was ignored whereas in the second simulation the bubble-bubble interaction was included. The emulsion phase density and viscosity were set to values that are common in polymerisation fluidised bed reactors. For the settings of the performed simulations see

. The time-averaged (over 190 s after 200 s) emulsion phase velocity profiles are presented in Figure 3.

Variable	Value
Emulsion density	400 kg.m^{-3}
Emulsion viscosity	0.1 Pa.s
Gas density	25 kg.m^{-3}
Initial bubble diameter	0.08 m
Superficial gas velocity	0.25 m.s^{-1}
Number of nozzles	49
NX	20
NY	20
NZ	60
Width	1.0 m
Depth	1.0 m
Height	3.0 m
Time step flowsolver	$5*10^{-3}$
Time step bubbles	$5*10^{-4}$
C_{vm}	0.5
C_d	2.67
Maximum bubble diameter	0.20 m

**Table 2:** Simulation settings.

The figure clearly shows that the bubble-bubble interactions have a profound influence on the macroscopic circulation patterns. When the bubble-bubble interactions are taken into account, the emulsion phase reaches its maximum velocity (corresponding to the maximum bubble diameter) already close to the gas distributor, indicating strongly enhanced bubble coalescence close to the distributor. The time-averaged porosity plots (Figure 4) and snapshots of the bubbles (Figure 4) show that the interaction forces tend to draw the bubbles towards the centre enhancing bubble coalescence. The predicted residence time of the bubbles in the bed is thus strongly decreased by the bubble-bubble interactions and the extent of the emulsion phase recirculation is increased considerably.

Figure 3: Influence of bubble-bubble interactions on the time-averaged emulsion phase velocity profiles: A) without bubble-bubble interactions; B) with bubble-bubble interactions (Farrokhalaee, 1979).
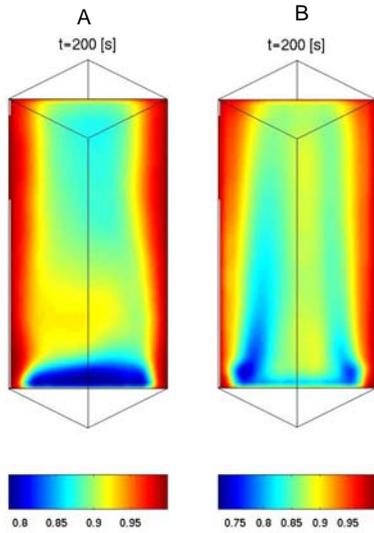
Figure 4: Influence of bubble-bubble interactions on the time-averaged porosity plots: A) without bubble-bubble interactions; B) with bubble-bubble interactions (Farrokhalaee, 1979).
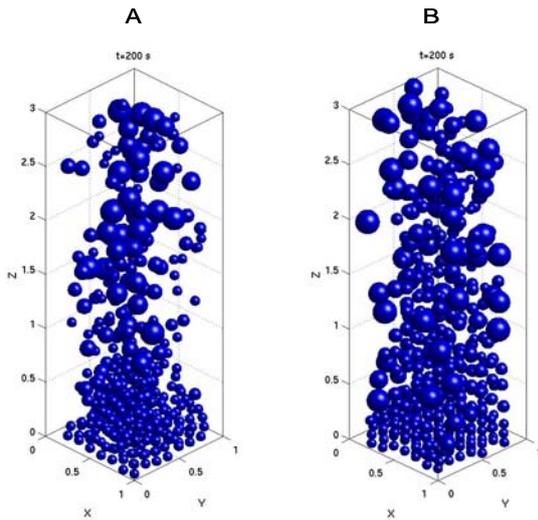

Figure 5: Influence of bubble-bubble interactions on snapshots of the bubbles after 200 s: A) without bubble-bubble interactions; B) with bubble-bubble interactions (Farrokhalaee, 1979).
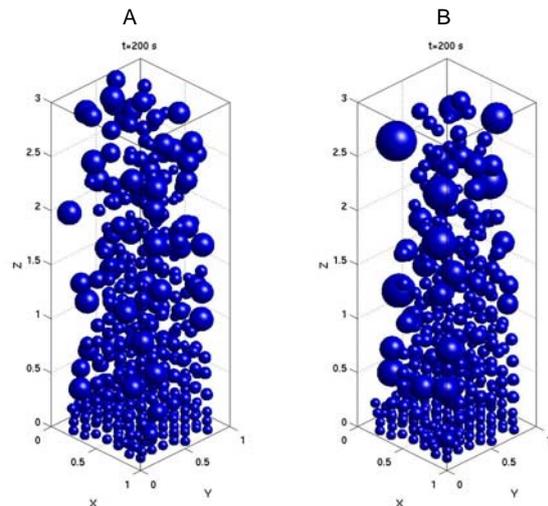
Influence of maximum bubble diameter

Since the maximum bubble diameter is reached already close to the gas distributor when accounting for the bubble-bubble interactions, the influence of the maximum bubble diameter on the macroscale circulation patterns has been studied. A simulation has been carried out by increasing the maximum bubble diameter from 0.2 m to 0.4 m, while keeping other simulation settings the same, see

. Figure 7 and Figure 7 shows the effect of the specified maximum bubble diameter on the time-averaged emulsion phase velocity profiles and on the bubble positions. With a larger maximum bubble diameter, the bubbles are drawn more to the centre of the fluidised bed, visualised in Figure 8, where the porosity is lower in the centre of the fluidised bed. This is cause by the enlarged bubble-bubble interaction area. In other words, the larger bubble attracts bubbles from a larger area, in addition, the larger bubbles will move faster through the fluidised bed explaining the increased emulsion phase velocity in the ascending flow. Moreover, the bigger the leading bubble the larger the interaction coefficients will be, increasing the velocity of the tailing bubble.
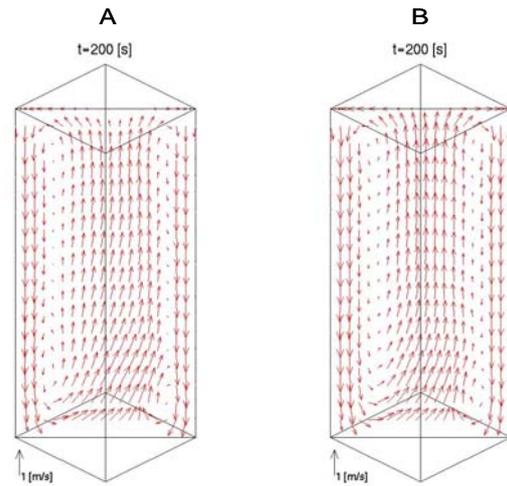
Figure 6: The time-averaged emulsion phase vector plots for both cases, the case with the small maximum bubble diameter is A) and the case with large maximum bubble diameter is B).

Figure 7: Snapshot of the bubbles, the case with the small maximum bubble diameter is A) and the case with large maximum bubble diameter is B).
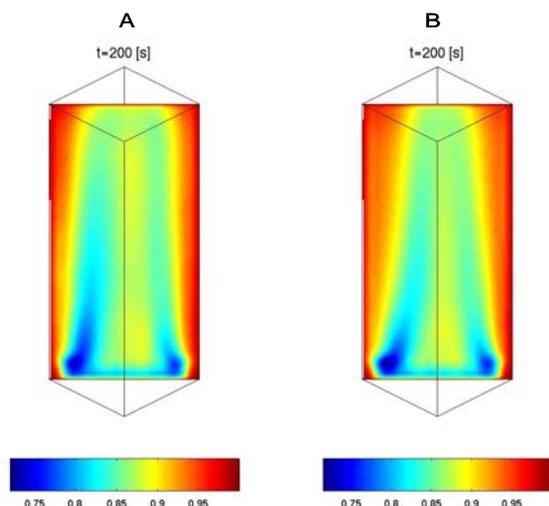
Figure 8: Time-averaged porosity plot. The case with the small bubble diameter is A) and the case with large maximum bubble diameter is B).

CONCLUSIONS

Binary bubble-bubble interaction forces have been incorporated in the DBM and a simulation study has been conducted to asses the effect on the macroscopic behaviour of freely bubbling fluidised beds. A large effect of the bubble-bubble interactions on the macroscopic circulation patterns and the bubble residence time was found. Due to the bubble-bubble interactions the emulsion phase reaches its maximum velocity much closer to the gas distributor, indicating strongly enhanced bubble coalescence, this is due to the fact that the bubbles are drawn towards the centre of the fluidised bed in a more pronounced way. With a larger maximum bubble diameter, the effects of the bubble-bubble interaction forces are even more pronounced. To validate the bubble-bubble interaction model, we are in the process of performing detailed Particle Image Velocimetry experiments.

ACKNOWLEDGMENT

REFERENCES

Auton, T. R. (1983). The dynamics of bubbles, drops and particles in motion in liquids, University of Cambridge.

Bokkers, G. A. (2005). Multi-level Modeling of Hydrodynamics in Gas Phase Polymerisation Reactors. Fundamentals of Chemical Reaction Engineering. Enschede, University of Twente.

Bokkers, G. A., J. A. Laverman, M. van Sint Annaland, J.A.M. Kuipers (2006). "Modelling of large-scale dense gas-solid bubbling fluidised beds using a novel Discrete Bubble Model." Chemical Engineering Science 61: 5590-5602.

Clift, R. and J. R. Grace (1971). "Coalescence of bubbles in fluidized beds." AIChE Symp. Ser 67(116): 23-33.

Clift, R. and J. R. Grace (1985). Continous Bubbling and Slugging. Fluidization. J. F. Davidson, R. Clift and Harrison. London, Acadamic Press.

Darmana, D., N. G. Deen, J.A.M. Kuipers (2005). "Detailed modeling of hydrodynamics, mass transfer and chemical reactions in a bubble column using a discrete bubble model." Chemical Engineering Science 60: 3383-3404.

Deen, N. G., M. van Sint Annaland, J.A.M. Kuipers (2004). "Multi-scale modeling of dispersed gas-liquid two-phase flow." Chemical Engineering Science 59: 1853-1861.

Farrokhalaee, T. (1979). "Gas distribution and bubble motion in fluidised beds." Ph.D. Thesis, Cambridge University, United Kingdom.

Krishna, R. and J. M. van Baten (2001). "Using CFD for scaling up gas-solid bubbling fluidised bed reactors with Geldart A powder." Chemical Engineering Science 82: 247-257.

Kuipers, J. A. M., K. J. van Duin, F.P.H. van Beckum, W.P.M. van Swaaij (1993). "Computer simulation of the hydrodynamics of a two dimensional gas-fluidized bed." Computational Chemical Engineering 17: 839.

Odar, F. and W. S. Hamilton (1964). "Forces on a sphere accelerating in a viscous liquid." Journal of Fluid Mechanics 18: 302-314.